The pairing condition itself implies that the structure factor of the observed reflection is zero. Therefore, we can conclude that the supposition of the previous section is false. No combination of symmetry elements can give rise to a pairing rule for an allowed reflection.

Summary and concluding remarks

In electron diffraction, it is difficult to use experimental intensities to solve crystal structures. This is because - unlike the case for X-rays - the intensity of a reflection does not depend only on the structure factor for that reflection but, through the complexities of dynamical diffraction, on many structure factors.

However, there are cases where the dynamical-diffraction multiple-diffraction routes can be shown to contribute nothing to the diffracted intensity. Unfortunately, these dynamical extinctions occur only when the structure factor for the observed reflection is itself zero.

Therefore, the idea that, by looking in specific circumstances and at a specific orientation, we could find an experimental intensity that would depend only on the structure factor for the observed reflection turns out not to be fruitful. The student asked a good question but one with an unhappy answer.

This conclusion should not be taken to mean that there are no methods of using electron diffraction intensities for crystal structure determination, only that the particular method proposed does not work. There are several ways of determining structure factors from electron diffraction. These have been reviewed by Gjønnes, Olsen & Matsuhata (1989) and Spence (1993). One of these methods in particular is related to the ideas of this paper: the Bristol group (Vincent & Exelby, 1994) has found situations where the intensities may be interpreted kinematically - although unfortunately only for high-order reflections.

I thank Jon Gjønnes for helpful comments. This work and the Center for Microanalysis of Materials are both supported by grant DEFG02-91ER45439 from the Department of Energy.

References

COWLEY, J. M. & MOODIE, A. F. (1959). *Acta Cryst.* **12**, 360-367.
COWLEY, J. M & MOODIE, A. F. (1962). *J. Phys. Soc. Jpn*, **17**, Suppl. BII, pp. 86-91.
COWLEY, J. M., MOODIE, A. F., MIYAKE, S., TAKAGI, S. & FUJIMOTO, F. (1961). *Acta Cryst.* **14**, 87-88.
EADES, J. A. (1988). *Microbeam Analysis*, pp. 75-80. San Francisco Press.
GJØNNES, J. & MOODIE, A. F. (1965). *Acta Cryst.* **19**, 65-67.
GJØNNES, J., OLSEN, A. & MATSUHATA, H. (1989). *J. Electron Microsc. Tech.* **13**, 98-110.
International Tables for Crystallography (1992). Vol. A. Dordrecht: Kluwer Academic Publishers.
MIYAKE, S., TAKAGI, S. & FUJIMOTO, F. (1960). *Acta Cryst.* **13**, 360-361.
SPENCE, J. C. H. (1993). *Acta Cryst.* A**49**, 231-260.
TANAKA, M. & TERAUCHI, M. (1985). *Convergent-Beam Electron Diffraction*. Tokyo: JEOL.
VINCENT, R. & EXELBY, D. (1994). *Philos. Mag.* In the press.

Acta Cryst. (1994). A**50**, 295–301

The Effect of a Crystal Monochromator on the Local Angular Divergence of an X-ray Beam

BY RICHARD D. SPAL

Ceramics Division, National Institute of Standards and Technology, Gaithersburg, MD 20899, *USA*

(*Received* 24 *February* 1993; *accepted* 1 *September* 1993)

Abstract

The performance of an X-ray optical system often depends critically on the local angular divergence of the X-ray beam. For example, in systems for radiography, tomography and diffraction topography, the angular divergence of the incident beam at a point in the sample determines the limiting spatial resolution. In this paper, formulas are derived for the local divergence in the diffracted beam of the non-dispersive asymmetric reflection double-flat-crystal monochromator, illuminated by synchrotron or characteristic radiation. The formulas are analyzed to determine the general behavior of the local divergence as a function of the asymmetry factors of the crystal reflections. For synchrotron radiation, one surprising conclusion is that the local divergence of the magnifying monochromator is always greater than that of the symmetric monochromator, significantly so for even moderate magnification factors. This result, which contradicts a claim in the literature, is attributed to a prismatic property of asymmetric reflection that has not previously been identified.

1. Introduction

A basic optical quantity that characterizes an X-ray beam is its local angular divergence, *i.e.* angular divergence at a given point. When the point is illuminated by a crystal monochromator, the local divergence will be determined by the characteristics of both the monochromator and the X-ray source. If only symmetric reflection is used, the effect of the monochromator is simple because symmetric reflection is formally equivalent to specular reflection for rays within the rocking-curve width; however, if asymmetric reflection is used, the effect is complex because asymmetric reflection can collimate or disperse rays within the rocking-curve width. In this paper, the non-dispersive asymmetric reflection double-flat-crystal monochromator is studied. A formula for the local divergence, involving the monochromator and source parameters, is derived and analyzed.

Some X-ray techniques are sensitive to the local divergence of the incident beam and benefit by its reduction. Prime examples are the projection imaging techniques of radiography, tomography and diffraction topography. Ideally, the local divergence of the incident beam is zero so that an object point is projected to a single image point. In practice, the local divergence is nonzero so that an object point is projected over an image area. Thus, the limiting spatial resolution of these imaging techniques is proportional to the local divergence of the incident beam at the object. Optimizing the spatial resolution clearly requires understanding of the local divergence.

Kuriyama, Boettinger & Burdette (1980) advocate a magnifying asymmetric reflection monochromator for radiography with characteristic radiation and Kuriyama, Steiner & Dobbyn (1989) advocate the same monochromator for diffraction topography with synchrotron radiation. In these two cases, they claim that the angular divergence of the monochromator's reflected beam is proportional to $m^{-1/2}$ and m^{-1}, respectively, where m is the magnification factor of the monochromator, and thereby conclude that increasing m improves collimation. However, they treat superficially the polychromaticity of the beam, so it is necessary to study the collimating effect of this monochromator more thoroughly.

Limited results concerning the local divergence may be obtained by elementary arguments, as follows. For simplicity, only the single-crystal monochromator is considered, although the treatment could easily be extended to the non-dispersive double-crystal monochromator. The monochromator is set at the Bragg angle θ_B for the wavelength λ_B using a reflection of absolute asymmetry factor $b = \sin(\theta_B - \alpha)/\sin(\theta_B + \alpha)$, where α is the angle between the crystal surface and reflecting atomic planes. Conventionally, b denotes the (signed) asymmetry factor, which is positive for Laue transmission and negative for Bragg reflection. However, since only the latter is treated in this paper, for convenience b is defined as the absolute value of the asymmetry factor. The rocking-curve width of the reflection is $b^{-1/2}\Omega_{\rm sym}$, where $\Omega_{\rm sym}$ is the rocking-curve width for symmetric reflection ($b = 1$) from the same atomic planes. The reflected beam is magnified by the factor b^{-1} so magnifying and demagnifying asymmetric reflection correspond to $b < 1$ and $b > 1$, respectively. The spectral width of the source is $\Delta\lambda$ and its angular divergence is $\Theta_{\rm src}$. For synchrotron radiation, $\Delta\lambda$ is large and $\Theta_{\rm src}$ is small; for characteristic radiation, the reverse holds. When the spectral width is small ($\Delta\lambda/\lambda_B << 1$), only incident rays in an angular range of $b^{-1/2}\Omega_{\rm sym} + (\Delta\lambda/\lambda_B)\tan\theta_B$ can satisfy the Bragg condition to within the rocking-curve width and therefore be reflected; all reflected rays are limited to an angular divergence of $b^{1/2}\Omega_{\rm sym} + (\Delta\lambda/\lambda_B)\tan\theta_B$. While the local divergence at an arbitrary point P in the reflected beam, denoted Θ_P, is most generally a solid angle, it is convenient to consider only those rays in the plane of diffraction of the monochromator, making it a planar angle.

In the absence of a monochromator, $\Theta_P = \min(\Theta_{\rm src}, \Theta_{P,\rm src})$, where $\Theta_{P,\rm src}$ is the angle at P subtended by the source. This may be extended to the symmetric reflection monochromator by constructing a point P', which is the mirror image of P through the crystal surface, as shown in Fig. 1. If symmetric reflection were equivalent to specular reflection for all rays, then Θ_P would equal $\min(\Theta_{\rm src}, \Theta_{P',\rm src})$. But they are only equivalent for rays within the rocking-curve width, so

$$\Theta_P = \min[\Theta_{\rm src}, \Theta_{P',\rm src}, \Omega_{\rm sym} + (\Delta\lambda/\lambda_B)\tan\theta_B].$$

Unfortunately, this result cannot be extended to the asymmetric reflection monochromator because asymmetric reflection is much more complex than specular reflection.

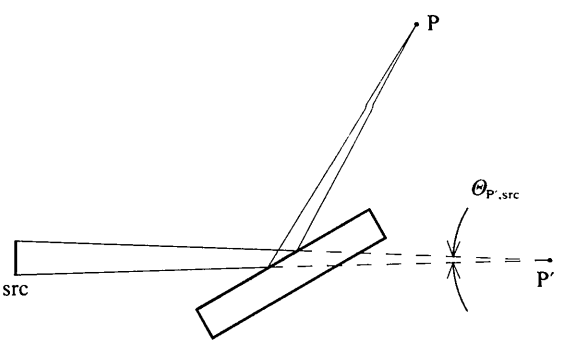

Fig. 1. Source-size contribution to local angular divergence for symmetric reflection.

For the asymmetric reflection monochromator, weaker results may be obtained in the form of inequalities that are useful in limiting cases. Clearly $\Theta_P \le b^{1/2}\Omega_{\rm sym} + (\Delta\lambda/\lambda_B)\tan\theta_B$, since all reflected rays, not only those intersecting at P, are confined to this angular range. Thus, in the limit of infinite magnification ($b = 0$) and ideal monochromaticity ($\Delta\lambda = 0$), the local divergence vanishes independently of source size. Another inequality may be obtained by regarding the crystal surface as a virtual source of limited size, which is viewed at a takeoff angle from P. Clearly $\Theta_P \le \Theta_{P,\rm src'}$, where $\Theta_{P,\rm src'}$ is the angle at P subtended by the virtual source. In the limit of infinite demagnification, the takeoff angle vanishes so the local divergence vanishes independently of the spectral width.

Derivation of the local divergence of the non-dispersive asymmetric reflection double-flat-crystal monochromator requires a complete mathematical description of the ray trajectories from the source through the monochromator to the observation point. In §2, these trajectories are obtained by the X-ray optical method of Matsushita & Kaminaga (1990) after convenient notation has been introduced. In §3, the local divergence is derived and analyzed.

2. Ray trajectories

To trace rays through the optical system, several coordinate systems are established, with origin O_0 at the center of the source, O_1 and O_2 at the center of the reflecting surface of the first and second crystal, respectively, and O_3 at an observation point centered in the reflected beam of the second crystal, as shown in Fig. 2. All the origins lie in the plane of diffraction of the monochromator, as do the coordinate systems, which are two dimensional since only rays in this plane are treated. The central ray, of wavelength λ_B, connects the four origins. At O_1 and O_2, the central ray bends by $2\theta_B$ and $-2\theta_B$, respectively, ignoring index-of-refraction corrections. Separate coordinate systems are established at O_1 for the incident and reflected beams, referred to by the subscripts $i1$ and $r1$, respectively. The positive z_{i1} and z_{r1} axes are directed from O_0 to O_1 and O_1 to O_2, respectively, *i.e.* along the incident and reflected central rays. The positive y_{i1} and y_{r1} axes are directed inside and outside the first crystal, respectively. In the same manner, two coordinate systems are established at O_2, referred to by the subscripts $i2$ and $r2$. Note that the $r1$ and $i2$ coordinate systems are parallel, *i.e.* $\hat{\mathbf{y}}_{r1} = \hat{\mathbf{y}}_{i2}$ and $\hat{\mathbf{z}}_{r1} = \hat{\mathbf{z}}_{i2}$. Finally, coordinate systems are established at O_0 and O_3, parallel to the $i1$ and $r2$ coordinate systems, respectively, referred to by the subscripts 0 and 3.

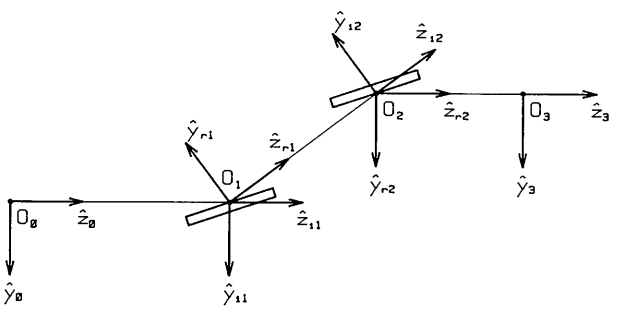

Fig. 2. Coordinate systems for a double-crystal monochromator.

Most generally, a ray is defined by a wave vector $\mathbf{k}$ and some point $\mathbf{r}$ on the ray; however, since all rays of interest lie near the central ray, it is convenient to use $(\mathbf{k} - \mathbf{k}_B)/|\mathbf{k}_B|$ instead of $\mathbf{k}$, where $\mathbf{k}_B$ is the wave vector of the central ray. (Technically, one of the above subscripts should be applied to $\mathbf{k}$ and $\mathbf{k}_B$ to specify a section of the optical system; however, since any subscript potentially applies, it is omitted for now.) The y and z components of $(\mathbf{k} - \mathbf{k}_B)/|\mathbf{k}_B|$ are denoted by y' and z', respectively. Since $\mathbf{k}_B$ is directed along $\hat{\mathbf{z}}$, y' is the angle between $\mathbf{k}$ and $\mathbf{k}_B$ and $z' = (\lambda_B - \lambda)/\lambda_B$, where λ is the wavelength of the ray. Note that z' differs in sign from the corresponding variable used by Matsushita & Kaminaga (1980), which they denote by $\Delta\lambda/\lambda_0$. The y and z components of $\mathbf{r}$ are denoted by y and z. However, it is convenient to chose $\mathbf{r}$ as the point on the ray for which $z = 0$. Thus, a ray is represented by the column vector $(y,y',z')^T$.

Ray propagation and reflection are described by transformations of ray coordinates between adjacent coordinate systems. Since the transformations are linear, they are represented by matrices. The propagation matrix between O_m and O_n, where $n = m + 1$, is

$$\mathbf{Z}_{nm} = \begin{bmatrix} 1 & z_{nm} & 0 \\ 0 & 1 & 0 \\ 0 & 0 & 1 \end{bmatrix},$$

where z_{nm} is the distance between the origins. An example of this transformation is $(y_{i1}, y'_{i1}, z'_{i1})^T = \mathbf{Z}_{10}(y_0, y'_0, z'_0)^T$. The reflection matrix for the nth crystal is

$$\mathbf{B}_n = \begin{bmatrix} b_n^{-1} & 0 & 0 \\ 0 & b_n & (b_n - 1)\tan\theta_B \\ 0 & 0 & 1 \end{bmatrix},$$

where b_n is the absolute asymmetry factor of the crystal. An example of this transformation is $(y_{r1}, y'_{r1}, z'_{r1})^T = \mathbf{B}_1(y_{i1}, y'_{i1}, z'_{i1})^T$. Matrix element $(\mathbf{B}_n)_{2,3}$ differs in sign from that in (3) of Matsushita & Kaminaga (1980) because z' differs in sign from their

corresponding variable, as noted above. The following transformations will be referred to later:

$$(y_{i1}, y'_{i1}, z'_{i1})^T = \mathbf{Z}_{10}(y_0, y'_0, z'_0)^T, \quad (1a)$$

$$(y_{i2}, y'_{i2}, z'_{i2})^T = \mathbf{Z}_{21}\mathbf{B}_1\mathbf{Z}_{10}(y_0, y'_0, z'_0)^T, \quad (1b)$$

$$(y_3, y'_3, z'_3)^T = \mathbf{Z}_{32}\mathbf{B}_2\mathbf{Z}_{21}\mathbf{B}_1\mathbf{Z}_{10}(y_0, y'_0, z'_0)^T. \quad (1c)$$

Physical interpretation of the equation $y'_r = by'_i + (b-1)\tan\theta_B z'_i$, contained in the reflection transformation, reveals the complexity of asymmetric reflection. For a monochromatic divergent incident beam, $y'_r = by'_i$, so the beam is collimated when $b < 1$ and dispersed when $b > 1$. This well known property led Kuriyama, Boettinger & Burdette (1980) and Kuriyama, Steiner & Dobbyn (1989) to advocate the magnifying asymmetric reflection monochromator for primary-beam collimation. For a polychromatic parallel incident beam, $y'_r = (b-1)\tan\theta_B z'_i$, so the beam is dispersed if $b \neq 1$. This prismatic property, not previously identified, is essential for understanding asymmetric reflection. Indeed, for the magnifying asymmetric reflection monochromator, this dispersive effect counteracts the collimation effect.

Mathematical approximation of the rocking curves and source (spatial, angular and spectral) distribution is required to obtain a simple formula for the local divergence. If the angular distribution of intensity at O_3 were strictly localized, meaning that it vanished everywhere outside some interval, then the local divergence would be conveniently defined as the width of the smallest such interval. Unfortunately, in practice, the distribution is not strictly localized but has long weak tails, owing to corresponding tails in the rocking curves and perhaps source distribution. Although the rocking curves are not strictly localized, they are nearly localized, meaning that almost all the area under each curve is confined to an interval not much larger than the full width at half-maximum (FWHM). Likewise, the source distribution is nearly localized, when not strictly localized. In the mathematical model below, these nearly localized functions have been approximated by strictly localized ones by cutting off their tails at the half-maximum points. While these points are somewhat arbitrary, another reasonable pair would only moderately alter the numerical value of the local divergence but would not change its general behavior as a function of the asymmetry factors and other parameters. As a result of the approximations, the angular distribution of intensity at O_3 is strictly localized and the local divergence is easily computed without the distribution itself having to be computed. Furthermore, the local divergence is independent of the details of the rocking curves and source distribution, depending only on their FWHM.

If the ray $(y_0, y'_0, z'_0)^T$ physically exists, it must satisfy the following constraints imposed by the source distribution:

$$|y_0| \le Y_0/2, \quad (2a)$$

$$|y'_0| < Y'_0/2, \quad (2b)$$

$$|z'_0| \le Z'_0/2, \quad (2c)$$

where Y_0 is the source's spatial FWHM, Y'_0 is its angular FWHM and Z'_0 is its spectral FWHM divided by the wavelength of the central ray ($\Delta\lambda/\lambda_B$). If the ray passes through the monochromator, it must satisfy two more constraints. First, it must lie within the rocking-curve widths of both crystals. Since $y'_{in} + \tan\theta_B z'_{in}$ is the angular deviation from the Bragg condition for a ray incident on the nth crystal, $|y'_{in} + \tan\theta_B z'_{in}| \le b_n^{-1/2}\Omega_{\rm sym}/2 \quad (n = 1, 2)$, where $\Omega_{\rm sym}$ is the FWHM of the rocking curve for symmetric reflection. With (1a) and (1b), these constraints are equivalent to

$$|y'_0 + \tan\theta_B z'_0| \le \Omega/2, \quad (3)$$

where $\Omega \equiv b_1^{-1/2}\min[1, (b_1b_2)^{-1/2}]\Omega_{\rm sym}$ is the effective rocking-curve width of the monochromator. Second, the ray must strike both crystal surfaces, which have finite length, so

$$|y_{in}| \le (L_n/2)\sin\theta_{in}, \quad n = 1, 2, \quad (4)$$

where L_n is the length of the nth crystal and $\theta_{in} \equiv \theta_B - \tan^{-1}[\tan\theta_B(1-b_n)/(1+b_n)]$ is the glancing angle of the beam incident on the crystal. This constraint could also be expressed in terms of y_0, y'_0 and z'_0 using (1a) and (1b). Finally, if the ray passes through O_3, where $y_3 = 0$, then, according to (1c),

$$0 = y_0 + [z_{10} + b_1^2 z_{21} + (b_1b_2)^2 z_{32}]y'_0 + [b_1(b_1-1)z_{21} + b_1b_2(b_1b_2-1)z_{32}]\tan\theta_B z'_0. \quad (5)$$

In conclusion, the rays that satisfy constraints (2)–(5) are exactly those that pass through O_3.

In three special cases, the double-crystal monochromator is equivalent, within the mathematical model, to a single-crystal monochromator of absolute asymmetry factor b, Bragg angle θ_B, rocking-curve width Ω, source-to-crystal distance $z_{\rm src}$ and crystal-to-observation-point distance z_P. First, if $b_1 \le 1$ and $b_2 = 1$, then the second crystal simply specularly reflects all incident rays so the two crystals are equivalent to one with $b = b_1$, $z_{\rm src} = z_{10}$ and $z_P = z_{21} + z_{32}$. Second, if $b_1 = 1$ and $b_2 \ge 1$, then the first crystal specularly reflects all rays that the second is capable of reflecting so the two crystals are equivalent to one with $b = b_2$, $z_{\rm src} = z_{10} + z_{21}$ and $z_P = z_{32}$. These two cases show that every single-crystal monochromator is equivalent to some double-crystal monochromator so it is unnecessary to treat the former separately. Third, if z_{21} is negligible compared to z_{10} and z_{32}, then $\mathbf{Z}_{21}$ may be approximated by the identity matrix, so $\mathbf{B}_2\mathbf{Z}_{21}\mathbf{B}_1 \simeq \mathbf{B}_2\mathbf{B}_1 = \mathbf{B}(b_1b_2)$, where

$\mathbf{B}(b_1b_2)$ is the reflection matrix with absolute asymmetry factor b_1b_2. Thus, the two crystals are equivalent to one with $b = b_1b_2$, $z_{\rm src} = z_{10}$ and $z_P = z_{32}$.

3. Local divergence

At O_3, according to (1*c*),

$$y'_3 = b_1b_2y'_0 + (b_1b_2 - 1)\tan\theta_B z'_0. \qquad (6)$$

As the ray $(y_0, y'_0, z'_0)^T$ varies throughout the region defined by constraints (2)–(5), y'_3 reaches a maximum value $Y'_3/2$ for some ray $(y_0^*, y'^*_0, z'^*_0)^T$. By symmetry, the minimum value of y'_3 in the region is $-Y'_3/2$ so Y'_3 is the angular divergence at O_3. The problem of finding Y'_3 and $(y_0^*, y'^*_0, z'^*_0)^T$ is an example of the well known linear-programming problem. At $(y_0^*, y'^*_0, z'^*_0)^T$, two of the inequality constraints (2)–(4) must be satisfied as equalities and are said to be active. These active constraints effectively determine the solution.

For different source and monochromator characteristics, different constraints may be active. However, in practice two cases are normally encountered. For synchrotron radiation, the local divergence is usually determined by the source size and the effective rocking-curve width so constraints (2*a*) and (3) are active. For characteristic radiation from a conventional tube, the local divergence is usually determined by the spectral width and the effective rocking-curve width so constraints (2*c*) and (3) are active. Characteristic radiation from a microfocus tube normally belongs to one of these cases. While only these two cases are treated below, additional ones could be treated by the same method.

In both cases, a formula for Y'_3 is given that was derived by re-expressing y'_3 [see (6)] in terms of the active constrained functions ($y'_0 + \tan\theta_B z'_0$ and y_0 or z'_0), using (5) as necessary to eliminate extraneous variables. In addition, formulas for evaluating the inactive constrained functions at $(y_0^*, y'^*_0, z'^*_0)^T$ are given for checking consistency. All inactive constraints should be satisfied. If an inactive constraint is violated, then the case does not apply and another case should be tried in which the violated constraint is active. Finally, the general behavior of Y'_3 with respect to the asymmetry factors is discussed and specific numerical examples are presented. Note that purely numerical results could have been more easily obtained by standard methods of linear programming, which systematically and efficiently consider as many cases as necessary to obtain the solution, or by ray-tracing programs; however, neither of these approaches is conducive to a general understanding of the influence of the asymmetry factors and other parameters on the local divergence. Of course, the present approach only yields the approximate width of the angular distribution of intensity at O_3. To obtain the distribution itself, a ray-tracing program is required to incorporate the details of the rocking curves and source distribution.

To facilitate discussion, the following abbreviated terminology is introduced to distinguish various monochromators according to b_1 and b_2. Symmetric (monochromator) refers to $b_1 = b_2 = 1$ and asymmetric to all other cases. Quasisymmetric refers to $b_1b_2 = 1$. Finally, magnifying and demagnifying refer to $b_1b_2 < 1$ and $b_1b_2 > 1$, respectively, and strictly magnifying and strictly demagnifying refer to $b_1 < 1$ and $b_2 < 1$ and $b_1 > 1$ and $b_2 > 1$, respectively.

3.1. *Synchrotron radiation*

In this case, the local divergence and inactive constraints are

$$Y'_3 = (Y_0 + |N|\Omega)/D, \qquad (7a)$$

where

$$N \equiv (1 - b_1b_2)z_{10} + b_1^2(1 - b_2)z_{21}$$

and

$$D \equiv z_{10} + b_1z_{21} + b_1b_2z_{32};$$

$$|Y_0 - \mathrm{sgn}\,(N)[(1 - b_1)z_{21} + b_2(1 - b_1b_2)z_{32}]b_1\Omega|/D \le Y'_0, \qquad (7b)$$

where $\mathrm{sgn}\,(N) \equiv N/|N|$ if $N \neq 0$;

$$|Y_0 + \mathrm{sgn}\,(N)[z_{10} + b_1^2z_{21} + (b_1b_2)^2z_{32}]\Omega|/D \le \tan\theta_B Z'_0; \qquad (7c)$$

$$b_1|(z_{21} + b_2z_{32})Y_0 + \mathrm{sgn}\,(N)[(1 - b_1)z_{21} + b_2(1 - b_1b_2)z_{32}]z_{10}\Omega|/D \le L_1\sin\theta_{i1}; \qquad (7d)$$

$$b_2z_{32}(Y_0 + |N|\Omega)/D \le L_2\sin\theta_{i2}. \qquad (7e)$$

If $N = 0$, $\mathrm{sgn}\,(N)$ may be fixed at any value from -1 to 1 in order to satisfy constraints (7*b*)–(7*d*).

Some numerical results of (7*a*), for various b_1 and b_2 with all other parameters fixed, are listed in Table 1, in order of increasing Y'_3. The values of the fixed parameters, also listed in Table 1, apply to the monochromator on beamline X23A3 of the National Institute of Standards and Technology, at the National Synchrotron Light Source, when set for $\lambda_B = 1.54$ Å using 111 reflections from silicon crystals. The values of Y_0 and Y'_0 refer to the source distribution in the plane of diffraction, which is perpendicular to the electron orbital plane. Since Z'_0 is effectively infinite, it is not listed. Of course, for the given b_1 and b_2, constraints (7*b*)–(7*e*) are satisfied. The values of b_1 and b_2 were selected to illustrate various points in the following discussion.

According to (7*a*), both the source size and the effective rocking-curve width contribute to the local divergence. However, since the latter contribution

Table 1. *Data for the synchrotron-radiation case*

Y_0	0.025 cm	L_1	5.0 cm
Y_0'	46.0″	L_2	5.0 cm
θ_B	14.22°	z_{10}	1705 cm
Ω_{sym}	7.0″	z_{21}	52 cm
		z_{32}	259 cm

b_1	b_2	b_1b_2	Y_3'(″)
22.891	0.437	10.000	0.940
1.000	1.000	1.000	2.558
0.100	10.000	1.000	2.671
0.316	3.162	1.000	2.674
10.000	1.000	10.000	3.302
0.100	9.000	0.900	4.548
3.162	3.162	10.000	5.754
1.000	0.100	0.100	9.101
1.000	10.000	10.000	9.239
0.316	0.316	0.100	13.908
0.100	1.000	0.100	22.536

includes the factor $|N|$, it vanishes when $N = 0$. In particular, it vanishes for the symmetric monochromator, implying that the rocking-curve-width contribution is purely an asymmetric reflection effect. This contribution can also vanish for the asymmetric monochromator, thereby yielding a small local divergence. Starting at the point (1, 1) in the b_1b_2 plane and following the curve $N(b_1, b_2) = 0$ in the direction of increasing b_1, both b_1 and b_1b_2 monotonically increase to infinity so Y_3' monotonically decreases to zero. Thus, the demagnifying monochromator can yield a smaller local divergence than the symmetric monochromator. Of course, this is expected from the elementary argument in §1. However, the demagnifying monochromator does not necessarily yield a smaller local divergence if $N(b_1, b_2) \neq 0$. For example, in Table 1, compare $Y_3'(1, 1)$ to the four $Y_3'(b_1, b_2)$ for which $b_1b_2 = 10$, noting that $N(22.891, 0.437) = 0$. Another example is the demagnifying single-crystal monochromator. As b increases from 1, (7*a*) implies that $Y_3'(1, b)$ monotonically decreases to zero if $\Omega_{sym} \leq (z_P/z_{src})Y_0/(z_{src} + z_P)$; if not, $Y_3'(1, b)$ initially increases before finally decreasing to zero. The latter is the case in Table 1; note that $Y_3'(1, 10) > Y_3'(1, 1)$.

In the region $0 \leq b_1 \leq 1$ and $0 \leq b_1b_2 \leq 1$, which includes all strictly magnifying monochromators but not all magnifying ones, $Y_3'(b_1, b_2)$ is minimized at (1, 1), since $|N|$ is minimized and D is maximized there. Thus, the local divergence of a magnifying monochromator in this region is always greater than that of the symmetric monochromator. For example, in Table 1, compare $Y_3'(1, 1)$ to the three $Y_3'(b_1, b_2)$ for which $b_1b_2 = 0.1$. Note that $Y_3'(b_1, b_2)$ can be much larger than Y_3' (1, 1). Since, as shown in §2, every single-crystal magnifying monochromator is equivalent to a monochromator in this region, the local divergence of any single-crystal magnifying monochromator is greater than that of the symmetric monochromator.

In the complementary region $b_1 \geq 1$ and $0 \leq b_1b_2 \leq 1$, which contains the remaining magnifying monochromators, (7*a*) implies that $Y_3'(b_1, b_2)$ is still minimized at (1, 1) if $Y_0/(z_{10} + z_{21} + z_{23}) \leq \Omega_{sym}$, as in Table 1. In any case, $Y_3'(b_1, b_2)$ monotonically decreases as b_2 increases at least until N vanishes, since $|N|$ monotonically decreases and D monotonically increases. But when $b_1 \geq 1$, N only vanishes for $b_1b_2 \geq 1$. Thus, the local divergence of a magnifying monochromator in this region is always greater than that of the quasisymmetric monochromator with the same b_1.

The results from these two regions imply that the local divergence of any magnifying monochromator is greater than that of the symmetric monochromator or the quasisymmetric monochromator with the same b_1. Thus, the magnifying monochromator has no special collimating effect for synchrotron radiation, in contrast to monochromatic radiation. Clearly, the prismatic effect of asymmetric reflection dominates the collimating effect.

For the quasisymmetric monochromator with $b_1 \leq 1$, if z_{21} is sufficiently small, then $D(b_1, b_1^{-1}) \simeq D(1, 1)$ and $|N|\Omega = b_1^{1/2}(1 - b_1)z_{21}\Omega_{sym} \simeq 0$, so $Y_3'(b_1, b_1^{-1}) \simeq Y_3'(1, 1)$. Although the magnifying first crystal would increase the local divergence acting alone, the demagnifying second crystal almost completely cancels the increase. Since z_{21} is almost negligible, this monochromator is nearly equivalent, as shown in §2, to the single-crystal monochromator with $b = b_1b_1^{-1} = 1$ and rocking-curve width $\Omega = b_1^{-1/2}\Omega_{sym}$, *i.e.* to the symmetric monochromator whose rocking-curve width is enhanced by the factor $b_1^{-1/2}$. Thus, this monochromator delivers a reflected beam $b_1^{-1/2}$ times more intense than that of the symmetric monochromator, ignoring reflectivity losses owing to absorption, with negligible increase in local divergence. Kohra, Ando, Matsushita & Hashizume (1978) previously noted the enhanced rocking-curve width of this monochromator. Although z_{21} may be negligible when $b_2 = b_1^{-1}$, it is not necessarily so when b_2 deviates slightly from this value. For example, in Table 1, compare $Y_3'(b_1, b_2)$ with $b_1b_2 = 1$ and $b_1b_2 = 0.9$. Note that a 10% change in b_2 produces an 80% increase in Y_3'.

3.2 *Characteristic radiation*

In this case, the local divergence and inactive constraints are

$$Y_3' = b_1b_2\Omega + \tan\theta_B Z_0', \tag{8a}$$

$$[z_{10} + b_1^2 z_{21} + (b_1b_2)^2 z_{32}]\Omega + (z_{10} + b_1z_{21} + b_1b_2z_{32})\tan\theta_B Z_0' \leq Y_0, \tag{8b}$$

$$\Omega + \tan\theta_B Z_0' \leq Y_0', \tag{8c}$$

$$b_1[(z_{21} + b_2^2 z_{23})b_1\Omega + (z_{21} + b_2 z_{32})\tan\theta_B Z_0'] \le L_1 \sin\theta_{i1}, \quad (8d)$$

$$b_2 z_{32}(b_1 b_2 \Omega + \tan\theta_B Z_0') \le L_2 \sin\theta_{i2}. \quad (8e)$$

According to (8*a*), Y_3' is a non-decreasing function of b_1 and b_2, with an absolute minimum of $\tan\theta_B Z_0'$ at $b_1 = b_2 = 0$. Thus, in this case, the local divergence of the magnifying monochromator is less than that of all others, and less than that of the symmetric monochromator by as much as Ω_{sym}. However, in practice, $\tan\theta_B Z_0'$ is much greater than Ω_{sym} so the impact of the magnifying monochromator is small. For Cu $K\alpha$ radiation, $Z_0' = 0.0029$, where the spectral width is taken as the separation of the most distant half-maximum points of $K\alpha_1$ and $K\alpha_2$. With Ω_{sym} and θ_B taken from Table 1, $\Omega_{sym}/(\tan\theta_B Z_0') = 0.05$, so only a 5% reduction in the local divergence is possible.

Finally, for each example in Table 1, the left side of constraint (7*c*) is less than 0.0029. Thus, if the lengths Y_0, z_{10}, z_{21} and z_{32} in Table 1 were reduced by the same factor, *e.g.* 10, in order to represent a monochromator with a microfocus tube, then the 'synchrotron-radiation' case would apply.

The previous results may be used to compute the spatial resolution of the Berg–Barrett method of diffraction topography by considering the specimen as a single-crystal monochromator. In this method, a highly magnifying asymmetric reflection is used, preferably with $2\theta_B$ near 90°. The film is placed parallel to the incident beam, making an angle θ_i with the specimen surface and touching it at an edge. This arrangement minimizes the distance z_P from a point on the specimen to its image on the film. If d is the distance from the specimen point to the line of intersection of the specimen surface and film, then $z_P = d\sin\theta_i/\sin 2\theta_B \simeq bd$. For a large source size, the spatial resolution, defined as $z_P Y_3'$, is $bd(b^{1/2}\Omega_{sym} + \tan\theta_B Z_0')$, from (8*a*), while for a small source size it is $bd[Y_0 + (1-b)z_{src}b^{-1/2}\Omega_{sym}]/(z_{src} + z_P) \simeq d(bY_0/z_{src} + b^{1/2}\Omega_{sym})$ from (7*a*). In both cases, the resolution improves as b decreases; in the second case, the improvement occurs despite increasing Y_3', owing to a more strongly decreasing z_P. Thus, the Berg–Barrett method is still advantageous after the local divergence is considered.

4. Summary

Ray trajectories for the non-dispersive asymmetric reflection double-flat-crystal monochromator, illuminated by an arbitrary X-ray source, are obtained by the X-ray optical method of Matsushita & Kaminaga (1980). The particular trajectory that determines the angular divergence at an observation point, centered in the reflected beam for convenience, is shown to be the solution of a linear-programming problem. This problem is solved for the two most practical cases, synchrotron and characteristic radiation, yielding formulas for the local divergence in terms of the monochromator and source parameters. These formulas are analyzed to determine the general behavior of the local divergence as a function of the asymmetry factors.

In the case of synchrotron radiation, the strictly magnifying monochromator always has greater local divergence than the symmetric one, a situation opposite that for ideally monochromatic radiation. This reversal is attributed to a prismatic property of asymmetric reflection. The intensity-enhancing quasi-symmetric monochromator has only slightly greater local divergence than the symmetric one. Finally, the demagnifying monochromator can have significantly less or greater local divergence than the symmetric one, depending on the asymmetry factors.

In the case of characteristic radiation from a conventional X-ray tube, the local divergence of the symmetric monochromator is always slightly greater than the magnifying one and always less than the demagnifying one. A microfocus tube may come under this case or the previous one, depending on the spot size.

References

KOHRA, K., ANDO, M., MATSUSHITA, T. & HASHIZUME, H. (1978). *Nucl. Instrum. Methods*, **152**, 161–166.

KURIYAMA, M., BOETTINGER, W. J. & BURDETTE, H. E. (1980). *Real-Time Radiologic Imaging: Medical and Industrial Applications*, ASTM Special Techincal Publication No. 716, edited by D. A. GARRETT & D. A. BRACHER, pp. 113–127. Philadelphia: American Society for Testing and Materials.

KURIYAMA, M., STEINER, B. W. & DOBBYN, R. C. (1989). *Annu. Rev. Mater. Sci.* **19**, 183–207.

MATSUSHITA, T. & KAMINAGA, U. (1980). *J. Appl. Cryst.* **13**, 472–478.